Strengthening Materials by Engineering Coherent Internal Boundaries at the Nanoscale

K. Lu, *et al.*

Science **324**, 349 (2009);
DOI: 10.1126/science.1159610

Science (print ISSN 0036-8075; online ISSN 1095-9203) is published weekly, except the last week in December, by the American Association for the Advancement of Science, 1200 New York Avenue NW, Washington, DC 20005.

Strengthening Materials by Engineering Coherent Internal Boundaries at the Nanoscale

K. Lu,[1]* L. Lu,[1,2] S. Suresh[2]*

Strengthening materials traditionally involves the controlled creation of internal defects and boundaries so as to obstruct dislocation motion. Such strategies invariably compromise ductility, the ability of the material to deform, stretch, or change shape permanently without breaking. Here, we outline an approach to optimize strength and ductility by identifying three essential structural characteristics for boundaries: coherency with surrounding matrix, thermal and mechanical stability, and smallest feature size finer than 100 nanometers. We assess current understanding of strengthening and propose a methodology for engineering coherent, nanoscale internal boundaries, specifically those involving nanoscale twin boundaries. Additionally, we discuss perspectives on strengthening and preserving ductility, along with potential applications for improving failure tolerance, electrical conductivity, and resistance to electromigration.

Classical methods for strengthening materials rely on strategies that judiciously control the generation of, and interactions among, internal defects. Such defects include: atomic vacancies and interstitials (point defects); dislocations (line defects); grain, interphase boundaries, and stacking faults that introduce crystallographic disregistry between adjacent regions of the atomic lattice (planar defects); and strengthening precipitates and dispersed reinforcement particles (volume defects) of a different phase or material than the surrounding matrix. Disruptions in a lattice strained by internal defects impede dislocation motion by which plastic deformation occurs, and this result translates into an enhanced macroscopic strength. Fig. 1, A and B, shows examples of several commonly used strengthening methods for crystalline metals and alloys. These approaches invariably suffer from the undesirable consequence that an increase in strength facilitated by dislocation interactions with internal barriers also causes reduced ductility and increased brittleness.

Motivation for Nanoscale, Coherent Internal Boundaries

The internal boundaries introduced by conventional strengthening methods (such as hardening by dispersed particles or grain refinement) are incoherent in that they do not create close crystallographic registry between regions separated by the boundaries, as shown in Fig. 1B for a boundary separating two adjoining grains. With strengthening achieved by introducing particles of a harder phase or material in a softer matrix, the mechanisms by which dislocations engender plasticity are strongly influenced by the size, shape, spatial distribution, and properties of the particles, as well as the geometry and deformation characteristics of particle-matrix interfaces. For grain refinement, the high concentration of incoherent grain boundaries (GBs) provides barriers to transmission of dislocations from one grain to the next (Fig. 1B). Although these high-energy, incoherent boundaries are effective in obstructing dislocation motion, their ability to accommodate plastic deformation is also compromised by reducing ductility (*1*). This makes the material harder to deform further, as informed by the Hall-Petch relationship for microcrystalline alloys (*2*). Strengthening with grain refinement is observed for grain sizes as small as ~10 to 15 nm (*3*–*6*). Activation of lattice dislocations at nano grain sizes becomes more difficult, and thus, plastic deformation becomes more limited. Therefore, nanocrystalline materials exhibit substantially increased strength and hardness (*1*, *3*, *4*). These materials also show higher loading rate sensitivity during plastic deformation (*7*, *8*), better tolerance to fatigue crack initiation under cyclic stressing, and greater resistance to deformation during normal indentation or frictional sliding as compared with microcrystalline materials (*9*–*12*). These beneficial attributes come at the expense of substantially lowered ductility (*1*) and resistance to stable fracture under monotonic and cyclic loading.

In contrast to GBs, coherent internal boundaries with low excess energies are seldom introduced as major strengthening agents for structural materials. Some coherent boundaries (such as low-angle tilt or twist GBs with aligned edge or screw dislocations, respectively) are not effective at resisting penetration by moving dislocations. Hence, their strengthening ability is relatively weak. Coherent internal boundaries created as precursors to the formation of strengthening precipitates in alloys hardened by heat treatments also offer possible means to strength enhancement. For example, the Guinier-Preston zones in precipitation-

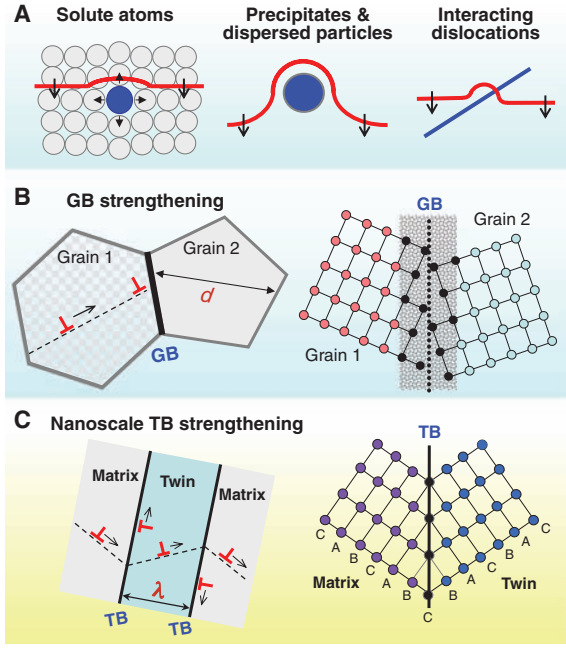

Fig. 1. Schematic illustration of examples of structural modifications for strengthening metals and alloys. Commonly used strengthening methods include (**A**) strengthening via solid solution, whereby solute atoms strain the matrix to impede the motion of a dislocation (red line) through the lattice; via precipitates or dispersed particles that interact with mobile dislocations, leading to overall strengthening of the material; or via elastic interactions between intersecting dislocations (blue and red lines), as well as geometry changes and subsequent obstructions to slip (as, for example, through the formation of sessile dislocation segments) associated with such encounters. GB strengthening (**B**) is another commonly used method in which dislocation (red ⊥ symbol) motion is blocked by GB (whose incoherent structure is schematically shown on the right) so that a dislocation pile-up is formed. A higher stress is needed to deform a polycrystalline metal with a smaller grain size *d* (more GBs). (**C**) Nanoscale TB strengthening is based on dislocation-TB interactions from which mobile and/or sessile dislocations could be generated, either in neighboring domains (twin or matrix) or at TBs. Gliding of dislocations along TBs is feasible because of its coherent structure [the right panel in (C) denotes a Σ3 TB]. Higher strength and higher ductility are achieved with a smaller twin thickness λ in the nanometer scale.

[1]Shenyang National Laboratory for Materials Science, Institute of Metal Research, Chinese Academy of Sciences, Shenyang 110016, China. [2]School of Engineering, Massachusetts Institute of Technology (MIT), 77 Massachusetts Avenue, Cambridge, MA 02139, USA.

*To whom correspondence should be addressed. E-mail: lu@imr.ac.cn (K.L.); ssuresh@mit.edu (S.S.)

hardenable Al-Cu alloys make up interfaces with the surrounding matrix that are easily penetrable by mobile dislocations (*13*). Another example involves the introduction of γ′ or γ precipitates in Ni-base superalloys and intermetallics intended for high-temperature applications (*2*). The thermal and mechanical stabilities of such zones are not sustained as precipitates grow in size and become increasingly incoherent with the surrounding matrix. In addition, the extent of strengthening achievable with such strategies is relatively limited, and even in cases of intermetallics where the extent of strengthening is acceptable, it is achieved at a major loss of ductility.

Internal boundaries can also be created within crystals by the introduction of twins. These planar defects form interfaces, one side of which contains arrangements of atoms that are mirror reflections of those on the other side separated by the twin composition plane, as schematically shown in Fig. 1C. Twin boundaries (TBs) within grains can be introduced either during processing (so called growth twins), plastic deformation (deformation twins), or recrystallization of deformed structures upon annealing (annealing twins). Compared with traditional high-angle GBs, TBs usually exhibit much higher thermal and mechanical stability. Strengthening of TBs is quantitatively identical to that of ordinary GBs (*14*), but strengthening from coherent TBs is relatively less pronounced than that from grain refinement when the TB spacing is of micrometer scale. Furthermore, the generation of a sufficiently high density of stable coherent (or semi-coherent) TBs for achieving even moderate strength enhancements is a technical challenge in the field of materials processing.

These considerations for designing material structures point to the need for strategies through which strengthening can be achieved for optimal mechanical performance in structural applications without compromising ductility and damage tolerance. Recent studies have shown that the controlled introduction of coherent, stable, and nanoscale internal boundaries offers the possibility for substantial strengthening while preserving acceptable levels of ductility, along with appealing electrical and thermal properties (*15*). Specifically, nanoscale twins that provide coherent internal interfaces within ultrafine-grained face-centered cubic (fcc) metals possess substantial strength. Unlike in conventional approaches, this marked increase in strength is not accompanied by a sharp reduction in ductility. Furthermore, when the twin thickness (the spacing between two adjoining twin boundaries) is taken as a characteristic structural dimension, analogous to the grain size, metals with coherent nanotwins exhibit comparable levels of yield strength, tensile strength, hardness, and strain rate sensitivity to deformation while still providing substantial ductility and work hardening when compared with the nanocrystalline metals of the same characteristic structural feature size (*15*–*18*).

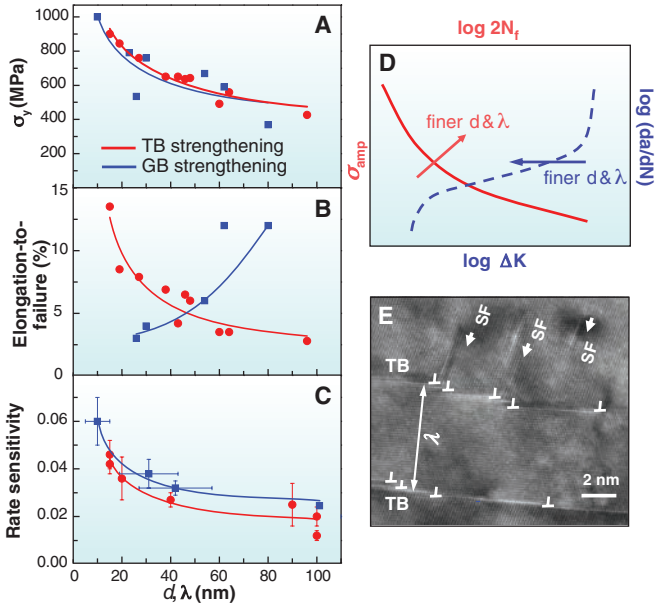

Fig. 2. Experimental results comparing the effectiveness of TBs in influencing mechanical properties with that of GBs for pure Cu. The characteristic structural dimensions used as a basis for comparison are λ and *d*. (**A**) Strength/hardness (σ_y), (**B**) elongation to failure, and (**C**) rate sensitivity of flow stress characterized by the parameter *m*. Error bars indicate ±SD from the mean of three samples. (**D**) Schematic illustration of the known effect of grain size *d* on stress-life fatigue response (left and top axes) characterized by the stress amplitude (σ_{amp}) and the number of stress reversals to failure ($2N_f$). Resistance to subcritical fatigue fracture characterized by the rate of fatigue crack growth (*da*/*dN*) versus the stress intensity factor range (Δ*K*) is plotted on a log-log scale on the bottom and right axes. Here, grain refinement generally leads to higher crack growth rates in the low- and mid-Δ*K* range. Similar behavior is anticipated for refinement of nanotwin thickness λ. (**E**) HRTEM image of the interaction of dislocations with nano TBs in pure Cu that had previously been deformed in tension. Arrows indicate the stacking faults (SF). Image reproduced with permission from (*19*).

Strategies for Strength Enhancements Without Severe Loss of Ductility

Figure 2A shows that for an ultrafine-grained Cu (grain size ~ 500 nm) with intragrain, nanoscale growth twins synthesized by pulsed electrodeposition, yield strength varies with twin thickness (λ) in the same manner as with grain size (*d*) for nanocrystalline Cu with incoherent GBs; both follow the empirical Hall-Petch relationship ($d^{-1/2}$ dependence) (*2*, *3*). Thus, nanoscale TBs impart as much strengthening as conventional high-angle GBs by blocking dislocation motion. Nanotwinned Cu also exhibits an elongation to failure of up to 14% at λ = 15 nm (*17*). A pronounced increment in tensile elongation to failure is observed with decreasing λ, in contrast to reduction in ductility at smaller *d* (Fig. 2B). The two characteristic structural dimensions λ and *d* influence the work-hardening response in very different ways. With a decrease in λ, a monotonic increase in work hardening occurs (*19*), in contrast to the near absence of work hardening in nano-grained fcc metals. This extraordinary work-hardening behavior demonstrates the unique strengthening effect of nanoscale TBs in contrast to that of GBs.

The effects of nanoscale TBs on strain rate sensitivity (*m*) in Cu have shown an increase in *m* with decreasing λ (Fig. 2C) (*16*). Here λ influences the rate sensitivity of deformation similarly to that by grain refinement in Cu and Cu alloys (*3*). Another measure of rate-controlling mechanism for plasticity is the activation volume (*v**); this quantity denotes the rate at which activation enthalpy decreases with yield stress at constant temperature. Experiments reveal a reduction in *v** from ~1000b^3 for microcrystalline fcc metals (*d* ~ 1 μm) without twins to ~10b^3 when either *d* or λ ~ 15 nm (here, *b* is the Burgers vector of Cu) (*16*).

Figure 2 implies that the presence of nanoscale TBs in ultrafine-grained Cu provides adequate barriers to dislocation motion for strengthening and creates more local sites for nucleating and accommodating dislocations, thereby elevating ductility and work hardening. These properties of nanotwinned materials originate from dislocation-TB interactions that differ fundamentally from the dislocation-GB interactions in nano-grained and coarse-grained metals.

In polycrystalline (nano-grained and coarse-grained) metals, GB strengthening results from impediment of GBs to dislocation motion. When a gliding dislocation encounters a GB, it is blocked, and a stress concentration is created at the dislocation-GB intersection. The localized stress concentration increases with an increasing number of incoming pile-up dislocations at a higher applied stress. When the stress concentration becomes large, new dislocations are nucleated on the other side of the GB in the neighboring grain, thereby eliminating the stress concentration at the GB. However, this process may not change the overall structure and energy state of the GB. Dislocation sliding is inhibited along GBs because of their disordered structures (as in Fig. 1B). Hence, the GBs have limited capacity to accommodate dislocations, resulting in a strength increase but a reduction in ductility.

Mechanistic models (*18*) ascribe increased strength and rate sensitivity in nanotwinned metals to the emission of partial or perfect dislocations into surrounding crystal from an existing boundary dislocation or site of stress concentration or crack in the sliding boundary. Continuum crystal plasticity models (*19*) of deformation in nanotwinned Cu invoke the possibility of softer

resistance to plastic flow and larger sensitivity to deformation rates within a small region (a few lattice parameters wide) of high dislocation density centered at the TB than that seen in elastic crystal lattice. These approaches also account for local plastic anisotropy with substantially easier shear deformation along the TBs than across them. With these assumptions, computational models correctly predict increased strength and rate sensitivity of nanotwinned Cu with finer twin thickness. If local failure is postulated to originate when a certain maximum slip deformation that can be accommodated by a TB is reached, these models reveal a qualitative trend of enhanced ductility with increasing twin density (*19*), consistent with experimental findings.

Atomistic simulations suggest that plastic response of nanotwinned metals is rate limited by slip transfer mechanisms as dislocations interact with TBs (*20*, *21*). As demonstrated systematically in (*20*), interactions between dislocations with a Σ3-TB (a special boundary with a coincident-site lattice separating two lattices with a particular misorientation so that one of every three sites is in coincidence) in different metals may result in glissile dislocations at the TB (i.e., twinning partials), sessile (immobile) dislocations or locks at the TB, and/or outgoing dislocations or stacking faults in the neighboring twin layer, depending on the nature of incoming dislocations. For instance, when an extended screw dislocation intersects a coherent TB in Cu under an applied stress, the dislocation can directly traverse across the TB with the incoming screw being absorbed into the TB and then desorbed through cross-slip (*20*) without any residual Burgers vector. Alternatively, direct transmission of the incoming extended screw dislocation can occur with the leading partial penetrating into the other side of the boundary. A sessile stair-rod dislocation temporarily develops on the TB until the trailing partial of the extended screw catches up.

These interactions could create sessile dislocations, stacking faults as well as steps along the TB, which can facilitate a loss of coherency (*20*). Figure 2E is a high-resolution transmission electron microscope (HRTEM) image of deformed nanotwinned Cu illustrating such a mechanistic process (*19*). The density of accumulated partial dislocations at TBs estimated from electron microscopy observations of deformed nanotwinned Cu is as high as 5×10^{16} m^{-2}, which is two orders of magnitude higher than that of lattice dislocations stored in coarse-grained Cu and much higher than that in the nanocrystalline Cu. Increasing TB density facilitates storage of these dislocations, thereby accommodating considerable strain hardening (*20*). Overall, high strength, rate-sensitivity of deformation, and improved ductility seen in nanotwinned fcc metals is attributed to the interaction between dislocation and a large number of initially coherent TBs, which gradually lose coherency as they harden during encounters with dislocations.

Apparently, coherent TBs may not only serve as sources and/or sinks of dislocations; they could also obstruct the transmission of dislocations from one side of the TB to the other. In addition, TBs may act as slip planes on which glissile dislocations can move and pile up; hence, the stress concentration at the dislocation-TB intersection may be effectively released by dislocation slip along TBs. This behavior allows accommodation of a considerable amount of plastic strain for a high density of TBs with a nanoscale TB spacing. Simultaneously, impediments to the easy flow of dislocations at the TBs and the continual loss of coherency contribute markedly to the enhancement in strength and ductility comparable to that of nanoscale grain refinement.

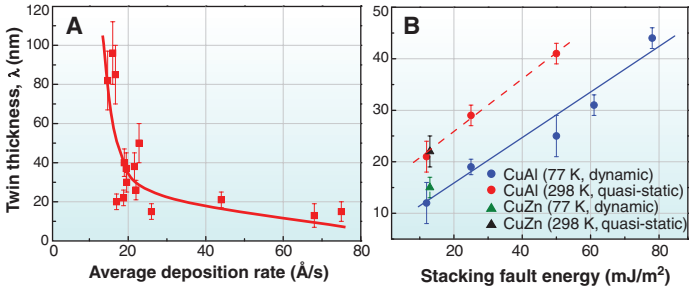

Fig. 3. Tailoring nanotwin thickness λ through control of pulsed electrodeposition processing parameters and material characteristics. Effects of (**A**) average deposition rate in Cu and (**B**) SFE in Cu alloys are shown. These alloys have been subjected to different plastic deformation processes by DPD at ~77 K (at a strain rate of 10^3 s^{-1}) and by quasi-static compression (at a strain rate of 10^{-3} s^{-1}) at room temperature (298 K) (*28*). Error bars indicate the standard measurement error from many TEM images on at least three individual samples.

Generation of Nanoscale Coherent Internal Boundaries

Coherent boundaries, including TBs and phase boundaries, can be generated through physical and chemical processes such as electrodeposition, sputter deposition, plastic deformation, recrystallization, and phase transformation. In electrodeposition of metals with appropriate stacking fault energies (SFEs), growth twins are frequently formed. As the propensity for twinning rises with deposition rate (Fig. 3A), pulsed electrodeposition is suitable for producing a high density of nanotwins (*15*). During the on period of pulsed deposition, a high transient deposition rate is induced by the high current density, resulting in a high density of twin nuclei and reduced twin thickness. During the off period, twin growth is interrupted.

Based on the imposed current density, nanotwins that are generated in ultrafine-grained pure Cu during pulsed electrodeposition—in which {111}/[112] type growth twins with mostly Σ3 coherent boundaries and some Σ9 boundaries—form parallel to the growth direction and extend through the grain. These edge-on twins formed in different crystals are oriented randomly around the foil normal (growth) direction. Twin thickness λ varies from a few nanometers to about 100 nm, depending on the deposition rate achieved by such processing parameters as current density, deposition temperature, and ratio of on time/off time (*17*). The formation of twins decreases total interfacial energy. Twins prefer to nucleate at GBs or triple junctions to reduce GB energies through orientation changes, and high twin density leads to lower average GB excess energy. Twin formation is kinetically driven, and the nucleation and growth rate of twins can be engineered by controlling deposition conditions and the nature of TBs and GB energy. Higher twin densities could be obtained in metals and alloys with low SFEs (e.g., Co and stainless steels) under the proper conditions.

By means of sputter deposition, nanoscale twins can be produced in various materials (*22*–*24*) at high deposition rates. When deposited on a substrate such as Si, GaAs, glass, or sapphire, thin films are grown with columnar grains in which coherent TBs evolve parallel to surface. As in electrodeposition, twin thickness decreases with increasing deposition rates; a minimum twin thickness of a few nanometers serves as the critical nucleus size that decreases substantially with an increase in deposition rate. Lower TB energies favor the formation of nanoscale twins. For materials with relatively higher TB energies such as Cu and Ni, sputtering at high deposition rates is needed to form high twin densities, whereas in alloys such as austenitic stainless steels with very low TB energies, high twin densities form at lower deposition rates of only a few nanometers per second. Large-scale production of nanotwinned copper foils (with diameter in centimeters) has been reported with the use of magnetron sputtering deposition (*25*).

Whereas these deposition processes produce thin foils with nanotwins, plastic deformation provides a practical approach to produce bulk metal and alloy specimens. Dislocation slip and deformation twinning are two competitive plastic deformation modes. Twinning is frequently observed in all body-centered cubic (bcc) metals and many fcc or hexagonal close-packed (hcp) metals when they are deformed at low temperatures and/or high strain rates, conditions that suppress dislocation motion. The size of deformation twins is controlled by their nucleation and growth kinetics, which depend on material characteristics [such as crystallographic structure, SFE, texture and grain size (*26*) and deformation conditions (strain, strain rate, and temperature)]. Twinning is easily achieved in bcc and hcp metals because of limited number of slip systems. In fcc metals with low SFEs [e.g., steels, Cu-Zn, and Cu-Al (*27*)], multiple twins are formed during deformation at conventional strain rates (<10° s^{-1}) and at ambient temperature. For those with higher SFEs such as

Cu and Ni, however, plastic deformation at high strain rates [i.e., dynamic plastic deformation (DPD)] and/or at lower temperatures is needed to induce twinning. Under the same deformation conditions, finer twins are formed in materials with lower SFEs, as shown in Fig. 3B. For the same material, twin density increases with increasing strain rates and/or lower temperatures (*28*).

Boundaries of deformation twins differ structurally from the coherent growth TBs or annealing TBs. High-density partial dislocations exist along deformation TBs, of which the excess energy is higher than that of fully coherent TBs. Upon further plastic straining, nanoscale deformation twins (usually in the form of bundles) may be transformed into nanosized grains via shear banding or fragmentation of twin/matrix lamellae. Then, the twin relationship across deformation TBs is destroyed by interaction with dislocations, forming high-angle GBs. Consequently, a composite structure is formed with nanoscale twin bundles embedded in nanosized grains (*29*).

Potential Applications and Challenges

A limited amount of published information appears to indicate that desirable electrical performance could also be achieved through the tailored creation of coherent nanoscale twins. Traditional strengthening approaches of metals and alloys generally promote a decrease in electrical and thermal conductivity, owing to an increase in scattering barriers. Thus, a tradeoff must be made between conductivity and mechanical strength. However, by introducing nanoscale coherent TBs in pure Cu, electrical conductivity is affected only slightly (comparable to that of coarse-grained high conductivity Cu), even though its mechanical strength increases by an order of magnitude (*15*). The combination of ultrahigh strength and high conductivity could possibly originate from the effective blockage of dislocation motion by numerous coherent nano-TBs with extremely low electrical resistivity, unlike other types of internal boundaries.

With reductions in feature size (well into the nanometer regime) of conducting metal lines in microelectronic circuits, high current densities result. The gradual migration of ions in a conductor from momentum transfer between diffusing metal atoms and conducting electrons leads to material transport. This causes depletion of material, which leads to voids and tensile stresses in the wake of electron transport, accumulation of material and formation of extruded regions (known as hillocks), and high compressive stresses at the opposite end. The ensuing failure process found in integrated circuits, which compromises their reliability, is commonly known as electromigration. Less-coordinated GBs within conducting metal lines are generally regarded as preferential electromigration paths. One recent study shows that by generating nanoscale twins within Cu grains, atomic transport at GBs driven by electrical current is reduced by an order of magnitude, possibly because of the presence of triple junctions of coherent TBs and GBs (*30*). Therefore, electromigration-induced failure of Cu lines in integrated circuits could be substantially suppressed when a high density of nanoscale TBs is introduced in Cu grains. Further experimental work is needed to elucidate the mechanisms underlying these effects.

Producing materials with nanoscale TBs in bulk form, which is essential to exploit their beneficial mechanical properties in structural applications, faces technical challenges. Electrodeposition is widely used to produce bulk metallic materials in industry. In principle, synthesizing bulk materials containing stable, coherent, nanoscale TBs by means of electrodeposition is feasible with proper deposition conditions. Optimization of deposition parameters and real-time closed-loop control of deposition kinetics are crucial for producing high deposition rates of twins during bulk processing. Copious coherent twins can be formed during recrystallization of deformed bulk metals upon annealing, driven by minimization of total excess energies of boundaries separating newly formed grains (*31*). The density of TBs depends on the number of new grain contacts made during recrystallization, as well as on their energy states. With proper plastic deformation followed by subsequent heat treatments, high density of coherent nanoscale TBs could be introduced in bulk metals (*32*).

Plastic deformation of metals at high strain rates and/or at cryogenic temperature provides practical approaches for producing materials in bulk form with nanoscale deformation twins (*29*). Bulk specimens comprising randomly oriented nanosized grains with embedded nanoscale twin bundles exhibit high strength and considerable ductility, owing to the strengthening from nanotwins and nanosized grains. Mechanical properties are determined by the concentration of nanotwin bundles, which varies greatly, depending on processing parameters and the material characteristics. Increased concentrations of nanotwin bundles can be achieved by optimizing initial crystallographic orientations (to favor twinning over slip) and/or suitable alloying to lower the SFE so that twinning is enhanced in each grain. The presence of high density of dislocations at TBs, characteristic of deformation twins, may lead to lower ductility compared with fully coherent TBs. Subsequent thermal and/or mechanical processes have been found to be effective in diminishing TB dislocations so that some plasticity is gained (*33*). Owing to the low energy state of TBs, the nanotwinned structures exhibit very high thermal stability and much better retention of strength upon annealing, as compared with nanocrystalline and ultrafine-grained metals (*34*). Annealing the nanotwin/nano-grain composite structure lead to recrystallization of the nano-grains, whereas the nanotwin bundles are retained. Such a composite structure with relative coarse grains (a few micron in size) embedded with nanotwin bundles would exhibit a good combination of high strength and ductility.

Another challenge is the applicability of these strategies to a broad variety of engineering materials. Whereas nanoscale twins form in many metallic materials, especially those with low SFE, some materials with high SFE (such as Al and Ni) may not easily form twins except under extreme conditions. Despite these challenges, the major gains in mechanical and physical characteristics and damage tolerance arising from the engineering of coherent internal boundaries in the nanoscale offer many potential opportunities in materials research and for engineering applications.

References and Notes

1. K. S. Kumar, H. V. Swygenhoven, S. Suresh, *Acta Mater.* **51**, 5743 (2003).
2. T. H. Courtney, *Mechanical Behavior of Materials* (McGraw-Hill, Boston, ed. 2, 2000).
3. J. Chen, L. Lu, K. Lu, *Scr. Mater.* **54**, 1913 (2006).
4. J. A. Knapp, D. M. Follstaedt, *J. Mater. Res.* **19**, 218 (2004).
5. C. A. Schuh, T. G. Nieh, H. Iwasaki, *Acta Mater.* **51**, 431 (2003).
6. H. Q. Li, F. Ebrihimi, *Acta Mater.* **54**, 2877 (2006).
7. R. Schwaiger, B. Moser, M. Dao, N. Chollacoop, S. Suresh, *Acta Mater.* **51**, 5159 (2003).
8. Q. Wei, S. Cheng, K.T. Ramesh, E. Ma, *Mater. Sci. Eng. A* **381**, 71 (2004).
9. T. Hanlon, Y.-N. Kwon, S. Suresh, *Scr. Mater.* **49**, 675 (2003).
10. A. B. Witney, P. G. Sanders, J. R. Weertman, *Scr. Mater. Mater.* **33**, 2025 (1995).
11. H. Mughrabi, H. W. Hoppel, *Mat. Res. Soc. Symp.* **634**, B2.1.1 (2001).
12. S. C. Bellemare, M. Dao, S. Suresh, *Mech. Mater.* **40**, 206 (2008).
13. J. Silcock, T. Heal, H. Hardy, *J. Inst. Met.* **82**, 239 (1953–1954).
14. W. J. Babyak, F. N. Rhines, *Trans. Met. Soc. AIME* **218**, 21 (1960).
15. L. Lu, Y. Shen, X. Chen, L. Qian, K. Lu, *Science* **304**, 422 (2004); published online 18 March 2004 (10.1126/science.1092905).
16. L. Lu *et al.*, *Acta Mater.* **53**, 2169 (2005).
17. Y. F. Shen, L. Lu, Q. H. Lu, Z. H. Jin, K. Lu, *Scr. Mater.* **52**, 989 (2005).
18. R. J. Asaro, S. Suresh, *Acta Mater.* **53**, 3369 (2005).
19. M. Dao, L. Lu, Y. Shen, S. Suresh, *Acta Mater.* **54**, 5421 (2006).
20. T. Zhu, J. Li, A. Samanta, H. G. Kim, S. Suresh, *Proc. Natl. Acad. Sci. U.S.A.* **104**, 3031 (2007).
21. Z. H. Jin *et al.*, *Acta Mater.* **56**, 1126 (2008).
22. X. Zhang *et al.*, *Acta Mater.* **52**, 995 (2004).
23. X. Zhang *et al.*, *Appl. Phys. Lett.* **88**, 173116 (2006).
24. S. K. Streiffer, E. M. Zielinski, B. M. Larison, J. C. Bravman, *Appl. Phys. Lett.* **58**, 2171 (1991).
25. A. M. Hodge, Y. M. Wang, T. W. Barbee, *Mater. Sci. Eng. A* **429**, 272 (2006).
26. X. L. Wu, Y. T. Zhu, *Phys. Rev. Lett.* **101**, 025503 (2008).
27. A. Rohatgi, K. S. Vecchio, G. T. Gray III, *Metall. Mater. Trans. A* **32**, 135 (2001).
28. Y. Zhang, N. R. Tao, K. Lu, *Scr. Mater.* **60**, 211 (2009).
29. Y. S. Li, N. R. Tao, K. Lu, *Acta Mater.* **56**, 230 (2008).
30. K.-C. Chen, W.-W. Wu, C.-N. Liao, L.-J. Chen, K. N. Tu, *Science* **321**, 1066 (2008).
31. J. E. Burke, D. Turnbull, *Prog. Mater. Sci.* **3**, 220 (1952).
32. M. Shimada, H. Kokawa, Z. J. Wang, Y. S. Sato, I. Karibe, *Acta Mater.* **50**, 2331 (2002).
33. Y. Zhang, N. R. Tao, K. Lu, *Acta Mater.* **56**, 2429 (2008).
34. X. H. Zhang, O. Anderoglu, R. G. Hoagland, A. Misra, *J. Met.* **60**, 75 (2008).

35. K.L. and L.L. are grateful for financial support of the National Natural Science Foundation (grants 50621091, 50431010, 50725103, and 50890171) and the Ministry of Science and Technology of China (grant 2005CB623604). L.L. and S.S. acknowledge support from the Office of Naval Research grant N00014-08-1-0510 and the Advanced Materials for Micro and Nano Systems Programme of the Singapore-MIT Alliance.

10.1126/science.1159610